

0040-4020(94)00587-7

SYNTHESIS AND PROPERTIES OF BILIRUBIN ANALOGS WITH *N,N*-METHYLENE BRIDGES

Ki-Oh Hwang, D. Timothy Anstine and David A. Lightner*

Department of Chemistry, University of Nevada
 Reno, Nevada 89557-0020 USA

Abstract. Bilirubin analogs have been prepared with a methylene group forming an *N* to *N* bridge. When the bridge is in the same dipyrinone, only one propionic acid can hydrogen bond intramolecularly (to the unbridged dipyrinone), but the pigment still adopts a ridge-tile conformation. Molecular dynamics calculations predict global energy minima for two enantiomeric ridge-tile conformations separated by an energy barrier of ~14.5 kcal/mole. In contrast, when the bridge connects two dipyrinones through their lactam nitrogens, that pigment is held in a porphyrin-like shape, neither propionic acid groups can participate in intramolecular hydrogen bonding, and the pigment is much more polar and hydrophilic than bilirubin. Molecular dynamics calculations predict an interconversion barrier of ~25 kcal/mole for this isomer.

INTRODUCTION

Complex linear tetrapyrroles such as the natural product bilirubin (Fig. 1A) are formed in animal metabolism from normal turnover of hemoglobin and other heme proteins.¹⁻³ Much effort has been devoted to understanding the properties and metabolism of bilirubin, which is the yellow, neurotoxic pigment of jaundice, and special attention has been focussed on its unique ability to fold into a conformation where the carboxylic acid groups are sequestered through intramolecular hydrogen bonding (Fig. 2A).⁴⁻⁶ Hydrogen bonding lowers their acidity, decreases the polarity of the pigment and renders it unexcretable in normal metabolism, except by glucuronidation. Bilirubin analogs with propionic acid groups relocated from their natural sites at C₈ and C₁₂ are more polar than bilirubin and do not require glucuronidation for hepatic excretion.^{7,8} But bilirubin analogs with propionic acid groups at C₈ and C₁₂, *e.g.*, mesobilirubin-XIII α (Fig. 1B), typically exhibit the same unique polarity and excretion properties because they too can tuck their carboxylic acid groups inward and tether them by intramolecular hydrogen bonding to their dipyrinones.

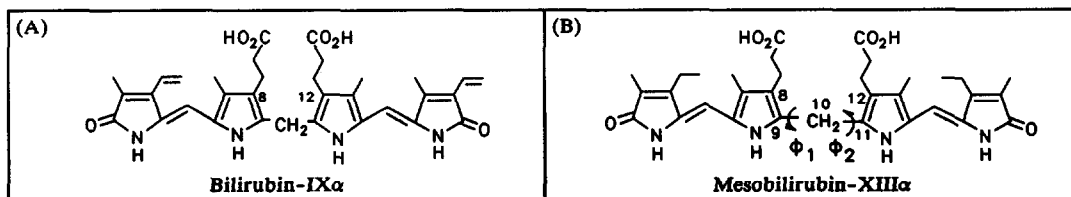


FIGURE 1. Linear Representations of (A) bilirubin-IX α and (B) mesobilirubin-XIII α . As shown in (B), the two dipyrinone chromophores may rotate independently about the central -CH₂- group (about torsion angles ϕ_1 and ϕ_2). Such rotations create a large number of conformations, only a few of which are stable.

Intramolecular hydrogen bonding is central to our understanding of bilirubin stereochemistry, solution properties and metabolism.^{3-7,9} Although the component dipyrirrones may rotate relatively freely and independently about the central $-\text{CH}_2-$ group to produce a large number of conformations, few have the unique ridge-tile shape required for intramolecular hydrogen bonding, *i.e.*, the structure shown in Figure 2A and its non-superimposable mirror image.⁶ These two enantiomeric conformations, despite stabilization from a network of intramolecular hydrogen bonds, are in dynamic equilibrium and interconvert fairly rapidly at room temperature over a barrier of ~ 20 kcal/mole.^{5,6} Our interest in defining the importance of intramolecular hydrogen bonding to pigment stereochemistry led us to consider tethering the lactam and pyrrole nitrogens (N_{21} and N_{22}) to a common alkyl chain as in Figure 2B. This can be expected to disrupt hydrogen bonds in one half of the molecule and thus allow us to assess the importance of intramolecular hydrogen bonding in the remaining half. By tethering both lactam nitrogens (Fig. 2C) or both sets of pyrrole nitrogens, intramolecular hydrogen bonding should become impossible, and these bilirubin analogs can thus be expected to exhibit very different solution and spectroscopic properties. In the following, we report on the synthesis, properties and conformational analysis of the unsymmetric N_{21},N_{22} -methanomesobilirubin-XIII α (1), and we compare these data with those of its isomer, N_{21},N_{24} -methanomesobilirubin-XIII α (2).

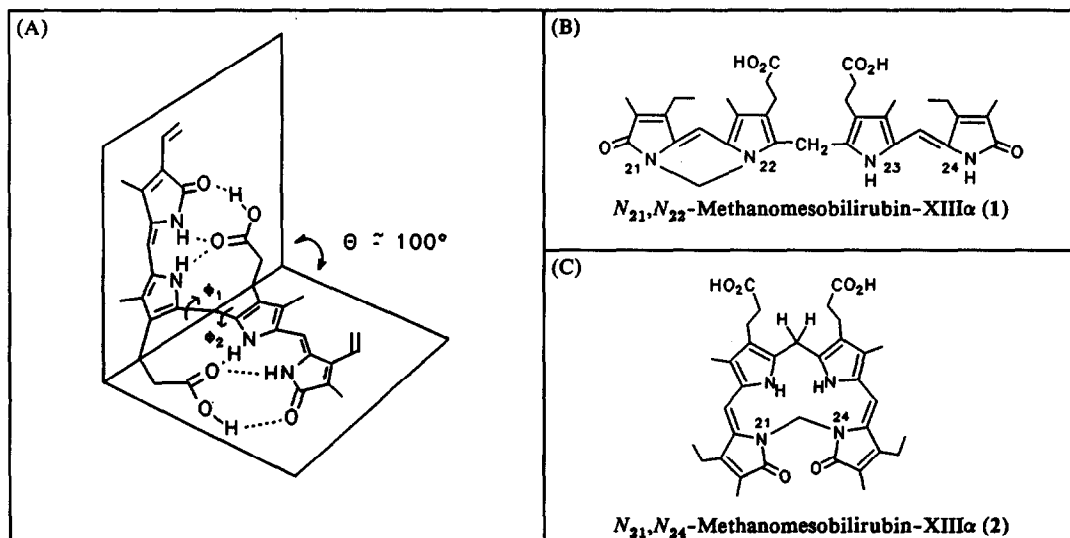


FIGURE 2. (A) Folded, intramolecularly hydrogen bonded conformation shaped like a ridge-tile and corresponding to a global energy minimum conformation. The interplanar dihedral angle $\theta \approx 100^\circ$, and $\phi_1 \approx \phi_2 \approx 60^\circ$, relative to $\theta \approx 0^\circ$ and $\phi_1 \approx \phi_2 = 0^\circ$ in the porphyrin-like conformation. Only one of two enantiomeric conformations is shown. (B) N_{21},N_{22} -Methanomesobilirubin-XIII α . (C) N_{21},N_{24} -Methanomesobilirubin-XIII α .

RESULTS AND DISCUSSION

Synthesis. Falk *et al.*¹⁰ showed previously that treatment of etioobiliverdin-IV γ with potassium hydroxide in dimethyl sulfoxide, followed by reaction with diiodomethane at relatively high temperature led to the formation of N,N -methano-bridged verdins (Fig. 3). In this particular reaction, three different methano-bridged verdins were isolated: N_{21},N_{22} ; N_{21},N_{24} and N_{22},N_{23} — with the last being a very minor product. In analyzing how this reaction might be directed to favor formation of either the N_{21},N_{22} or the N_{21},N_{24} isomer, we

thought that the base strength might influence the product ratio because the pK_a values of pyrrole and lactam hydrogens differ. Thus, when etiobiliverdin was treated with sodium methoxide (pK_a of conjugate acid ~ 16) in *N,N*-dimethylformamide, the product of methenylation with methylene diiodide was mainly the N_{21},N_{24} verdin (25%), with only a minor amount (1-2%) of the N_{21},N_{22} isomer being formed. No N_{22},N_{23} isomer was detected. Sodium methoxide was used in the successful conversion of mesobiliverdin-XIII α ¹¹ to its N_{21},N_{24} -methano analog (7), which was converted to rubin 2 (Scheme 1).¹² In contrast, when dimethyl lithium (from methyl lithium in dimethyl sulfoxide) was used as a base (pK_a of dimethyl sulfoxide ~ 33),

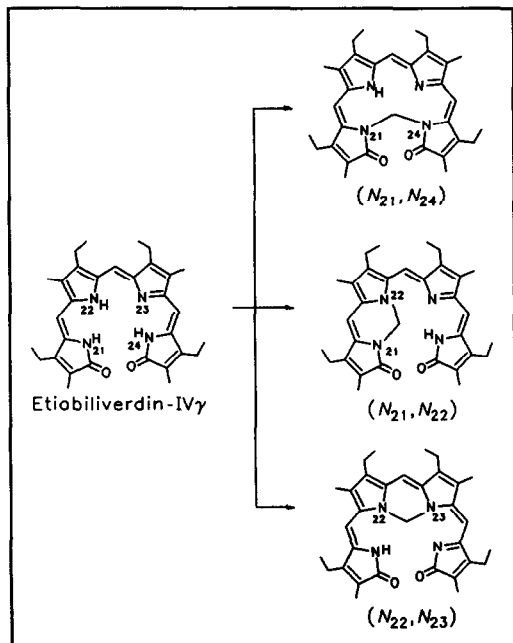


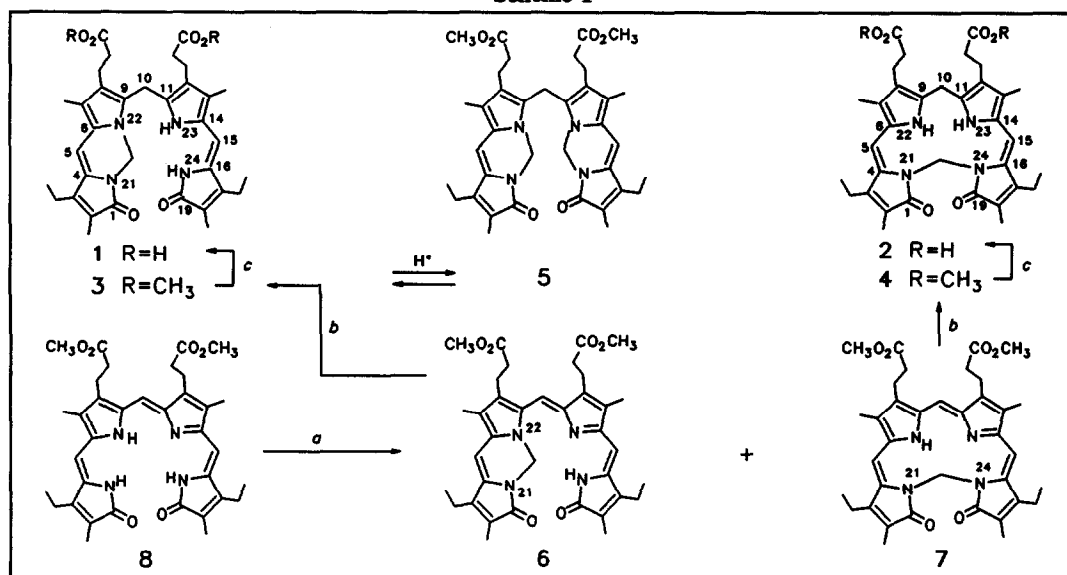
FIGURE 3. Synthesis of *N,N'*-methanoetiobiliverdins according to Falk *et al.* (ref. 11).

the N_{21},N_{22} bridged verdin was the major isomer (10-13%) with little or none of the other isomers. In this rather clean, low yield method, the target, N_{21},N_{22} -methanomesobilirubin-XIII α (1), was prepared in three steps from mesobiliverdin-XIII α dimethyl ester (8) as outlined in Scheme 1. Thus, the N_{21},N_{22} -methano-bridged verdin analog (6) was prepared in 13% yield along with less than 1% of the N_{21},N_{24} isomer (7) as a by-product. Reduction of 6 to the corresponding rubin dimethyl ester (3) was achieved in 75% isolated yield by action of sodium borohydride in tetrahydrofuran-isopropyl alcohol. Rubin ester (3) is quite unstable in acid; however, and unless the acidic work-up is carried out at low temperature and the pH kept above 3, disproportionation¹ takes place to yield a mixture of 3, 5 and mesobilirubin-XIII α dimethyl ester. Although not surprising, formation of the interesting doubly bridged rubin ester 5 was an unintended bonus. Saponification of 3 to give diacid 1 was achieved in refluxing 10% ethanolic sodium hydroxide. These conditions are more severe than

those normally required for the saponification of rubin esters, but when the reaction was carried out at 50°C in tetrahydrofuran or tetrahydrofuran-methanol, only a mono-acid was formed.

Polarity from Chromatographic Behavior. N_{21},N_{22} -methanomesobilirubin-XIII α (1) has a shorter retention time (~ 11.8 minutes) when coinjected with the parent mesobilirubin-XIII α (~ 17.3 minutes) on reverse phase HPLC,¹³ suggesting that 1 is more polar than the parent. And on silica gel TLC, 1 has a smaller R_f value (~ 0.7) when compared with the mesobilirubin-XIII α standard ($R_f \sim 0.9$) using $CHCl_3:CH_3OH$ (100:3, vol/vol) as eluant, confirming that 1 is somewhat more polar. These chromatographic results may be compared with those of the corresponding dimethyl esters. The retention times for 3 (~ 5.1 minute) and mesobilirubin-XIII α dimethyl ester (~ 5.2 minute) are quite comparable on reverse phase HPLC, and the TLC retention times the same ($R_f \sim 0.4$) — data indicating that acids are less polar than the esters. This behavior is consistent with the acid polarity being decreased by intramolecular hydrogen bonding. In contrast, the HPLC retention time of 2 is shorter (~ 5.5 minute) than 1 and on silica gel TLC, the R_f is ~ 0 .

Scheme 1



^a CH₂I₂/(CH₃)₂SO + CH₃Li; ^b NaBH₄/(CH₃)₂CHOH-tetrahydrofuran; ^c NaOH.

TABLE 1. Comparison of the ¹³C-NMR Chemical Shifts and Assignments for N₂₁,N₂₃-Methanomesobilirubin-XIII α (1), and Mesobilirubin-XIII α , and N₂₁,N₂₄-Methanomesobilirubin-XIII α (2) in (CD₃)₂SO.^a

Position	Carbon	δ for 1	δ for Meso-bilirubin-XIII α	δ for 2
1/19	C=O	167.9/172.0	172.4	169.4
2/18	=C-	123.2/122.7	123.0	118.5
2 ¹ /18 ¹	CH ₃	8.62/9.08	9.62	9.52
3/17	=C-	147.3/143.5	141.7	146.2
3 ¹ /17 ¹	CH ₂	17.04/17.12	17.64	17.44
3 ² /17 ²	CH ₃	14.83/14.61	15.29	14.77
4/16	=C-	128.8/128.2	128.3	127.6
5/15	=CH-	97.64/97.70	98.19	99.13
6/14	=C-	122.2/121.2	122.4	121.4
7/13	=C-	119.6/118.8	119.72	119.67
7 ¹ /13 ¹	CH ₃	8.09/8.14	8.54	8.14
8/12	=C-	124.2/123.3	123.4	123.8
8 ¹ /12 ¹	CH ₂	19.27/19.37	19.74	19.78
8 ² /12 ²	CH ₂	34.24/34.53	34.81	35.60
8 ³ /12 ³	C=O	173.7/174.0	174.5	174.3
9/11	=C-	129.0/129.3	130.8	136.2
10	CH ₂	21.73	23.96	22.28
N,N'	-CH ₂ -	54.58	—	54.82

^a Run at 2.5 x 10⁻² M concentration of pigment at 22°C. Chemical shifts are in ppm downfield from (CH₃)₄Si.

Structure from NMR. The constitutional structures of the N_{21},N_{22} and N_{21},N_{24} -methano-rubins **1** and **2** are consistent with their ^{13}C -NMR (Table 1). Thus, for N_{21},N_{22} -methanomesobilirubin-XIII α (**1**), the carbon chemical shifts show the expected doubling due to dissymmetrization of the mesobilirubin-XIII α structure by bridging the pyrrole and lactam nitrogens of only one dipyrri- none. On the other hand, the N_{21},N_{24} isomer has the same symmetry and nearly the same chemical shifts as the parent mesobilirubin-XIII α . Both **1** and **2** show a new carbon signal from the N-CH₂-N bridge. Although the chemical shifts of the carbons in the β -substituents are nearly the same in mesobilirubin-XIII α **1** and **2**, somewhat larger differences may be noted in comparing certain carbon chemical shifts of the tetrapyrrole nucleus. Such differences probably reflect changes in shieldings due to the presence of the N-CH₂-N bridge, which restricts the shape of **2** to a new helical conformation, one very different from that of the unbridged parents. For example, carbon 10 in **1** and **2** are shielded by ~ 2 ppm relative to those of mesobilirubin-XIII α .

NMR Analysis and Intramolecular Hydrogen Bonding. In bilirubins, the ^1H -NMR *N-H* chemical shifts of the pyrrole and lactam have proven to be an excellent way to determine whether the dipyrri- none units of bilirubins are involved in intramolecular hydrogen bonding.^{14,15} Previous studies have shown that the carboxylic acid COOH appears near 13.5 δ and the lactam and pyrrole *N-H*'s appear near 10.6 and 9.2 δ , respectively, in CDCl₃ solvent (*e.g.* for mesobilirubin-XIII α of Table 2) when the dipyrri- none and carboxylic acid groups are intramolecularly hydrogen bonded, as shown in Figure 2.^{14,15} When the propionic acids are esterified, however, the pyrrole hydrogens become more deshielded (10.3 δ) due to dipyrri- none-dipyrri- none intermolecular hydrogen bonding (Table 2).^{3,16} In (CD₃)₂SO, the dipyrri- none *N-H*'s become hydrogen bonded to solvent; so, the distinctions seen in CDCl₃ are lost, and all pyrrole *N-H* resonances appear near 10.4 δ . The data for **1** follow the behavior of mesobilirubin-XIII α in CDCl₃ and in (CD₃)₂SO, suggesting that its unbridged dipyrri- none is involved in a similar sort of intramolecular hydrogen bonding. Whether the greater shielding of the pyrrole *N-H* of **1** in CDCl₃ is due to a weaker *N-H* hydrogen bond or to a shielding influence from the bridged dipyrri- none is unclear. The data suggest that **1** probably adopts a conformation similar to that found in Figure 2A, but with only half the complement of hydrogen bonds. In contrast, the conformation of **2** is held in a helical porphyrin-like shape by the N_{21},N_{24} -methano-bridge. The pyrrole NH's of **2** are not expected to become involved in hydrogen bonding, and thus their chemical shifts are relatively more strongly shielded in CDCl₃. In (CD₃)₂SO solvent, however, the chemical shifts are much less strongly shielded (Table 2), suggesting that this solvent hydrogen bonds to the pyrrole *N-H*'s even in a sterically crowded environment.

TABLE 2. Comparison of Bridged and Unbridged Mesobilirubin Lactam and Pyrrole *N-H* Chemical Shifts^a in CDCl₃ and (CD₃)₂SO Solvents.^b

Pigment	CDCl ₃			(CD ₃) ₂ SO		
	Lactam	Pyrrole	CO ₂ H	Lactam	Pyrrole	CO ₂ H
N_{21},N_{22} -Methanomesobilirubin-XIII α (1)	10.81	8.15	13.60 11.99	9.78	10.37	11.97
Mesobilirubin-XIII α	10.57	9.15	13.62	9.72	10.27	11.87
N_{21},N_{24} -Methanomesobilirubin-XIII α (2)	—	7.89 ^c	insol.	—	9.64	12.06
N_{21},N_{24} -Methanoetiobilirubin-IV γ	—	7.39	—	—	9.6	—

^a δ , ppm downfield from (CH₃)₄Si. ^b 10⁻² M (CD₃)₂SO and 10⁻³ M CDCl₃ solutions at 22°C. ^c Dimethyl ester due to insolubility of free acid in CDCl₃.

UV-Visible Spectral Analysis and Conformation from Exciton Coupling. Additional evidence on the conformation of **1** comes from solvent-dependent UV-visible spectra. Over a wide range of solvents with varying polarity and hydrogen bonding ability (benzene, chloroform, methanol and dimethylsulfoxide), the UV-visible spectra of **1** and mesobilirubin-XIII α are very similar (Table 3), changing very little, with λ^{\max} being near 430 nm and λ^{sh} near 395 nm^{11,16} — corresponding to the two exciton components from electric transition dipole-dipole interaction of the two proximal dipyrinone chromophores approximately 90° apart (as in Fig. 2A).^{6,16} Since mesobilirubin is known from NMR studies to adopt the intramolecularly hydrogen bonded conformation of Figure 2A in CDCl₃ solvent and a similar conformation in (CD₃)₂SO solvent,⁵ it might be argued that a UV-visible exciton couplet with $\lambda^{\max} \approx 430$ nm, $\lambda^{\text{sh}} \approx 395$ nm can be taken as an indicator of a folded (but not necessarily hydrogen-bonded) conformation akin to that of Figure 2A. In contrast, the UV-visible spectra of **2** (Table 3) exhibit an observed λ^{\max} shifted to the blue by 40-50 nm and ϵ^{\max} reduced by 50% or more. This blue shift is expected from exciton coupling theory^{17,18} when the pigment adopts a conformation in which the dipyrinone component chromophores are oriented with nearly parallel transition dipoles. The data for **2** are thus fully consistent with a porphyrin-like conformation (Fig. 2C); whereas, the data for **1** are consistent with a folded ridge-tile shape.

TABLE 3. Comparison of UV-Visible Spectral Data^a for *N*₂₁,*N*₂₂-Methanomesobilirubin-XIII α (**1**) and *N*₂₁,*N*₂₄-Methanomesobilirubin-XIII α (**2**) With Mesobilirubin-XIII α .

Solvent	UV-Visible λ^{\max} (ϵ^{\max})		
	1	Mesobilirubin-XIII α	2
C ₆ H ₆	432 (38,500)	435 (52,100)	381 (20,400)
CH ₂ Cl ₂	426 (40,800)	431 (53,200)	396 (22,800)
CHCl ₃	427 (38,000)	431 (52,800)	390 (19,800)
(CH ₃) ₂ CO	426 (38,200)	428 (50,400)	378 (20,100)
CH ₃ CN	421 (36,500)	425 (49,300)	377 (20,700)
CH ₃ OH	420 (37,100)	426 (51,600)	384 (23,100)
	403 (37,800)	401 ^{sh} (43,300)	
(CH ₃) ₂ SO	416 (33,000)	426 (49,300)	385 (23,800)
	396 (40,500)	397 ^{sh} (47,200)	

^a Run at 1-2 x 10⁻⁶ M concentrations; λ^{\max} and λ^{sh} in nm; ϵ^{\max} and ϵ^{sh} in L · mole · cm⁻¹.

As might be expected, the UV-visible spectra of the bridged dimethyl esters are quite different from that of mesobilirubin-XIII α dimethyl ester (Table 4). Very little solvent dependence is found (Table 4) among **3**, **4** and **5**. In contrast, mesobilirubin-XIII α dimethyl ester exhibits a strong solvent, concentration and temperature dependence due to formation of dimers^{3,19} in non-polar solvents, such as benzene and chloroform, that exhibit a narrow bandwidth intense absorption with λ^{\max} near 380 nm and weak shoulder at λ^{sh} near 430 nm.^{11,16} In more polar solvents such as CH₃OH and (CH₃)₂SO the solutions are largely monomeric, and the UV-visible spectra are thus quite similar to those of the parent acid in these solvents, with λ^{\max} near 435 nm and λ^{sh} near 400 nm.^{10,15a} The *N*₂₁,*N*₂₂ ester **3** shows none of these characteristic shifts and exhibits a nearly solvent-independent exciton couplet (~415 nm, ~395 nm) in the UV-visible absorption. The dimethano bridged ester (**5**) also shows very little solvent dependence, with a wavelength-shifted exciton couplet near 435 and 415 nm. In marked contrast the *N*₂₁,*N*₂₄ ester (**4**) exhibits a weaker absorption

near 378-385 nm. Its UV-visible spectrum provides corroborating evidence for porphyrin-like structures, as the UV-visible λ^{\max} are blue shifted, as is expected for an exciton system where the component chromophores are positioned such that the relevant electric transition moments approach the parallel alignment. In a folded conformation (Fig. 2A) or a linear conformation, the transition moments are not parallel, and the UV-visible maximum is red-shifted.¹⁹ The UV-visible spectra of **3** and **4** are similar and point to the prevalence of conformations where the pigment lies in a folded or stretched conformation.

TABLE 4. Comparison of UV-Visible Spectral Data^a of the Dimethyl Esters of *N*₂₁,*N*₂₂-Methanomesobilirubin-XIII α (**3**), *N*₂₁,*N*₂₄-Methanomesobilirubin-XIII α and *N*₂₁,*N*₂₂:*N*₂₃,*N*₂₄-Dimethanomesobilirubin-XIII α (**5**) With Mesobilirubin-XIII α Dimethyl Ester.

Solvent	UV-Visible λ^{\max} (ϵ^{\max})			
	3	4	Mesobilirubin-XIII α Dimethyl Ester	5
C ₆ H ₆	397 (38,500)	381 (21,000)	380 (60,700)	417 (34,600)
	412 (39,300)			438 (34,600)
CH ₂ Cl ₂	394 (37,500)	382 (21,400)	376 (62,600)	412 (34,000)
	409 (37,500)			431 (34,000)
CHCl ₃	407 (39,000)	379 (20,900)	382 (59,300)	417 (33,900) 433 (34,000)
(CH ₃) ₂ CO	388 (39,300)	378 (23,700)	377 (51,500)	408 (35,000)
	413 (35,000)			429 (34,900)
CH ₃ CN	389 (51,100)	379 (22,100)	374 (60,400)	406 (35,100)
	405 (47,700)		422 ^{sh} (15,600)	427 (34,800)
CH ₃ OH	396 (41,700)	383 (26,000)	396 ^{sh} (42,400)	403 (37,800)
	420 (36,000)		428 (57,500)	412 (35,400) 431 (34,200)
(CH ₃) ₂ SO	415 (42,400)	385 (26,500)	396 ^{sh} (42,800)	414 (35,300)
	419 (36,100)		430 (61,500)	436 (34,500)

^a Run at $1-2 \times 10^{-5}$ M concentrations; λ^{\max} and λ^{sh} in nm; ϵ^{\max} and ϵ^{sh} in L · mole · cm⁻¹.

Conformational Analysis from Molecular Dynamics Calculations. Additional insight may be gained from an analysis of pigment conformation by molecular dynamics methods using the force field in SYBYL. Conformational energy maps⁶ can be constructed by rotating the dipyrinone units independently about the C9-10 and 10-11 carbon-carbon single bonds (Scheme 1), corresponding to torsion angles ϕ_1 and ϕ_2 , respectively. The conformational energy map (Fig. 4) of **1** is qualitatively similar to that of the parent, mesobilirubin-XIII α ,⁶ and the minimum energy conformation adopted by **1** is rather like that of the parent, mesobilirubin-XIII α , despite the fact that only one dipyrinone can participate in intramolecular hydrogen bonding. (The other has no NH groups due to the *N*₂₁-CH₂-*N*₂₂ bridge.) The most stable ridge-tile structure is thus dissymmetric, with $\phi_1 = 60^\circ$ and $\phi_2 = 30^\circ$ for the *P*-helicity conformation. In mesobilirubin-XIII α , $\phi_1 = \phi_2 = 61^\circ$, but its interplanar dihedral angle ($\theta = 96^\circ$) and that of **1** ($\theta = 99-102^\circ$) are quite similar. The *P* and *M*-chirality conformers of **1** interconvert over a barrier of ~ 14.5 kcal/mole — compared with ~ 20 kcal/mole for mesobilirubin-XIII α .^{5,6} Unlike mesobilirubin-XIII α , **1** displays local minima (Fig. 4) nearby the global minima, but lying some 11 kcal/mole higher in energy. The local minima correspond to isoenergetic homomeric or enantiomeric conformations that are more extended and flatter than the ridge-tile global minimum energy conformations.

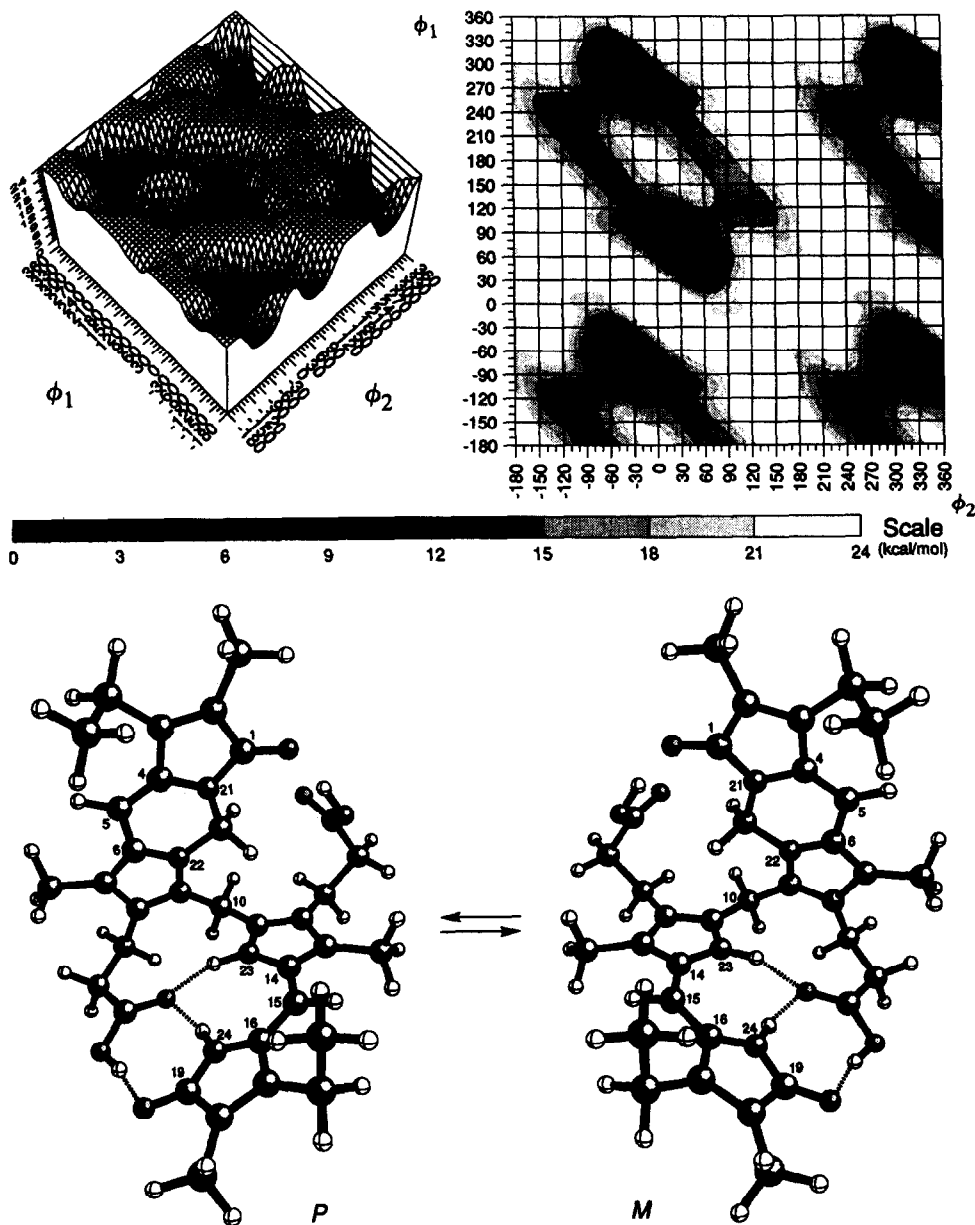


FIGURE 4. (Upper Left) Potential energy surface and (Upper Right) contour map for N_{21},N_{22} -Methanomesobilirubin-XIII α (1) conformations generated by rotating the two dipyrinone groups independently about the C_9-C_{10} and $C_{10}-C_{11}$ bonds (ϕ_1 and ϕ_2 respectively). The energy scale (Middle) is in kcal/mol, and global minima (set to 0 kcal/mol) are found near $(\phi_1, \phi_2) \simeq (60^\circ, 30^\circ)$ (*P*-chirality), and $(\phi_1, \phi_2) \simeq (-60^\circ, -30^\circ)$, $(-60^\circ, 330^\circ)$, $(300^\circ, -30^\circ)$, $(300^\circ, 330^\circ)$ (*M*-chirality). Local minima are found at $(\phi_1 = \phi_2) \simeq (120^\circ, 120^\circ)$ (*P*-chirality) and $(\phi_1 = \phi_2) \simeq (-120^\circ, -120^\circ)$, $(-120^\circ, 240^\circ)$ (*M*-chirality). Data are from molecular dynamics simulations using SYBYL $^{\circledR}$ (Tripos Assoc.) on an Evans & Sutherland ESV-10 workstation. (Lower) Ball and stick conformational representations for the ridge-tile shape *M* and *P*-chirality intramolecularly hydrogen bonded, interconverting enantiomers of 1. Drawings from Müller and Falk's "Ball and Stick" program (Cherwell Scientific, Oxford, U.K.) for the Macintosh.

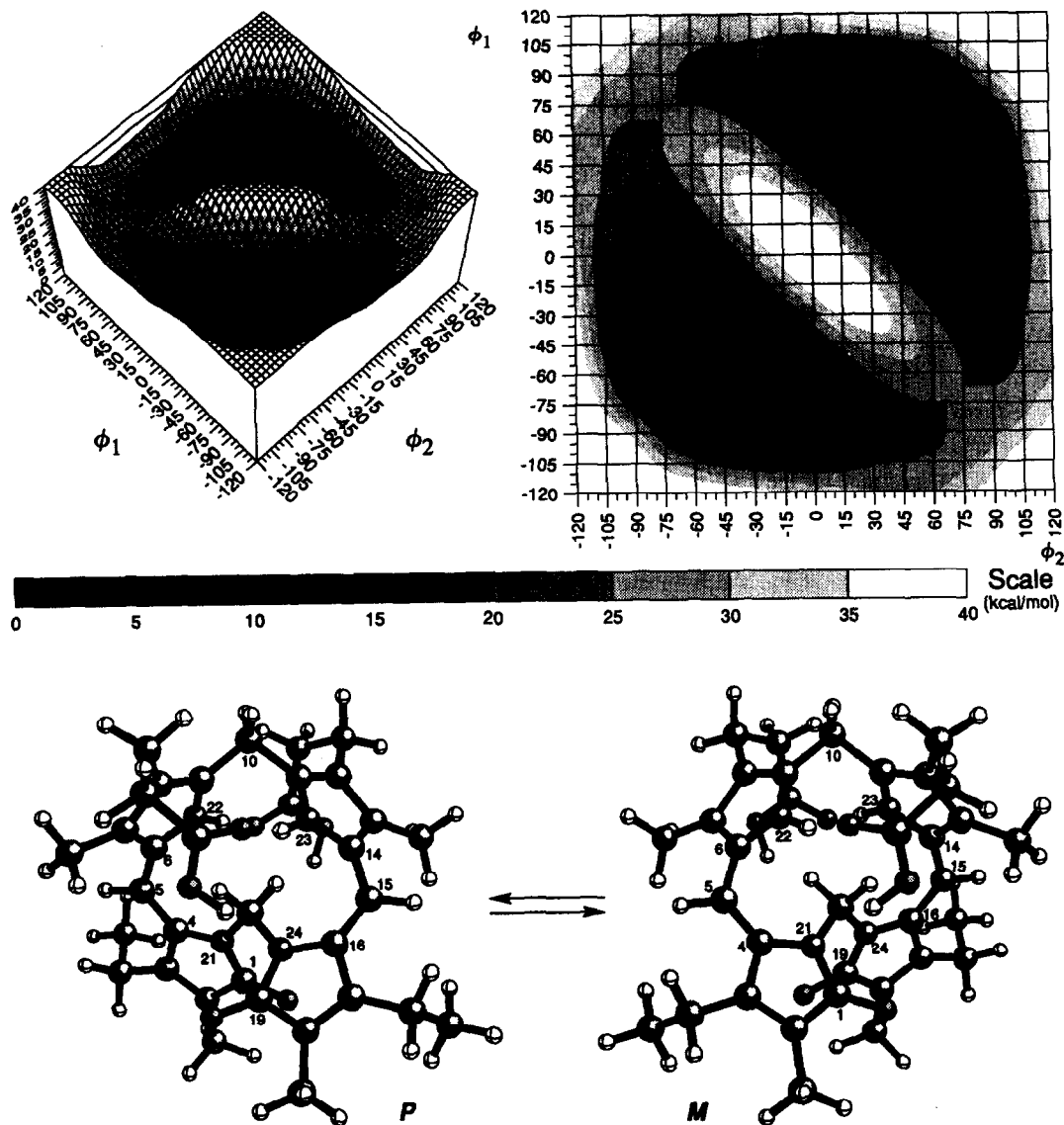


FIGURE 5. (Upper Left) Potential energy surface and (Upper Right) contour map for N_{21},N_{24} -Methanomesobilirubin-XIII α (2) conformations generated by rotating the two dipyrinone groups independently about the C_9-C_{10} and $C_{10}-C_{11}$ bonds (ϕ_1 and ϕ_2 respectively). The energy scale (Middle) is in kcal/mol, and global minima (set to 0 kcal/mol) are found near $(\phi_1, \phi_2) \simeq (50^\circ, 50^\circ)$ (*P*-chirality), and $(\phi_1, \phi_2) \simeq (-50^\circ, -50^\circ)$ (*M*-chirality). Data are from molecular dynamics simulations using SYBYL[®] (Tripos Assoc.) on an Evans & Sutherland ESV-10 workstation. (Lower) Ball and stick conformational representations for the ridge-tile shape *M* and *P*-chirality intramolecularly hydrogen bonded, interconverting enantiomers of 2. Drawings from Müller and Falk's "Ball and Stick" program (Cherwell Scientific, Oxford, U.K.) for the Macintosh.

In stark contrast, **2** does not exhibit intramolecular hydrogen bonding, and its conformation is constrained by the N_{21} -CH₂-N₂₄ bridge. The conformational energy map (Fig. 5) shows that only a limited array of conformations can be created by rotations about ϕ_1 and ϕ_2 , due to the constraints imposed by the N_{21} -CH₂-N₂₄ bridge. The most stable of these are shown in Figure 5. Two global minima located near $\phi_1 = \phi_2 = +50^\circ$ and $\phi_1 = \phi_2 = -50^\circ$ correspond to the mirror image structures of Figure 4. Here, unlike bilirubin, the dipyrinone units are severely twisted, with C₄-C₅-C₆-N₂₂ and N₂₃-C₁₄-C₁₅-C₁₆ torsion angles of 57° , compared to only a few degrees in the folded intramolecularly hydrogen bonded ridge-tile structure of Figure 2A. The molecular conformation is thus highly twisted, with a dihedral angle of 107° between the two pyrroles flanking C₁₀ and a dihedral angle of 52° between the average planes of the dipyrinones flanking C₁₀. Rotations about ϕ_1 and ϕ_2 interconvert the enantiomeric structures of **2** over an activation barrier estimated by molecular dynamics to be ~ 25 kcal/mole.

Induced Circular Dichroism and Binding to Albumin. As may be seen in Figure 6, a solution of **1** in buffered solution with 2 mole equivalents of human serum albumin (HSA) gives a bisignate circular dichroism (CD) spectrum for the long wavelength UV-visible transition. The CD is similar to but much weaker in magnitude than that observed for mesobilirubin-XIII α . In contrast, **2** shows only a weak, oppositely-signed CD. When bound to HSA and other albumins, bilirubin-IX α is known to exhibit optical activity, seen typically as an intense and bisignate induced circular dichroism (CD).^{20,21} The origin of the optical activity comes from the pigment adopting a chiral conformation selected at the binding site on the protein. The observed bisignate CD comes from exciton coupling of two electric dipole transitions: one from each of the pigment's twin dipyrinone chromophores, *viz.* those from the long wavelength UV-visible excitation near 410 nm. The protein acts as an enantioselective binding agent and constrains the pigment to adopt a chiral conformation, and as reported previously,²⁰ the presence of at least one propionic acid group at C₈ or C₁₂ is essential to the enantioselectivity in binding. These CD data may be contrasted with those induced by association with (-)-ephedrine and quinine (Table 5), where much more intense bisignate Cotton effects may be seen for **1** and mesobilirubin-XIII α , but only weak bisignate Cotton effects are seen with **2**.

TABLE 5. Comparison of Circular Dichroism and UV-Visible Spectral Data^a for N_{21},N_{22} -Methanomesobilirubin-XIII α (**1**), Mesobilirubin-XIII α , and N_{21},N_{24} -Methanomesobilirubin-XIII α (**3**) in: (A) pH 7.4 Buffered Aqueous Human Serum Albumin Solutions Containing 1% Dimethylsulfoxide,^b (B) Chloroform Plus (1*R*,2*S*)-(-)-Ephedrine,^c and (C) Dichloromethane Plus Quinine.^d

Pigment	Circular Dichroism			UV-Visible
	$\Delta\epsilon_{\max}(\lambda_1)$	λ at $\Delta\epsilon=0$	$\Delta\epsilon_{\max}(\lambda_2)$	$\epsilon_{\max}(\lambda)$
N_{21},N_{22} -Methanomesobilirubin-XIII α (1)	(A) +21 (453)	408	-3.6 (398)	40,500 (406)
	(B) ^e -89 (445)	419	+68 (401)	41,000 (430)
	(C) ^d -110 (436)	409	+67 (389)	42,200 (429)
Mesobilirubin-XIII α	(A) +35 (444)	408	-35 (392)	43,000 (435)
	(B) -110 (447)	419	+87 (402)	40,000 (438)
	(C) -120 (445)	418	+92 (400)	41,500 (437)
N_{21},N_{24} -Methanomesobilirubin-XIII α (2)	(A) -4.7 (422) ^e	386	+3.7 (366)	16,000 (378)
	(B) -15 (422)	383	+4.8 (357)	16,300 (378)
	(C) -16 (410)	370	- ^e	16,200 (377)

^a $\Delta\epsilon$ and ϵ in L \cdot mole⁻¹ \cdot cm⁻¹ and λ in nm. ^b For $2-3 \times 10^{-5}$ M pigment solutions run with 2 mole equivalents of human serum albumin, 1% (CH₃)₂SO has no effect on the BR-HSA CD spectrum. ^c 1000:1 molar ratio amine:pigment. ^d 500:1 molar ratio amine:pigment. ^e Overlapped with quinine band.

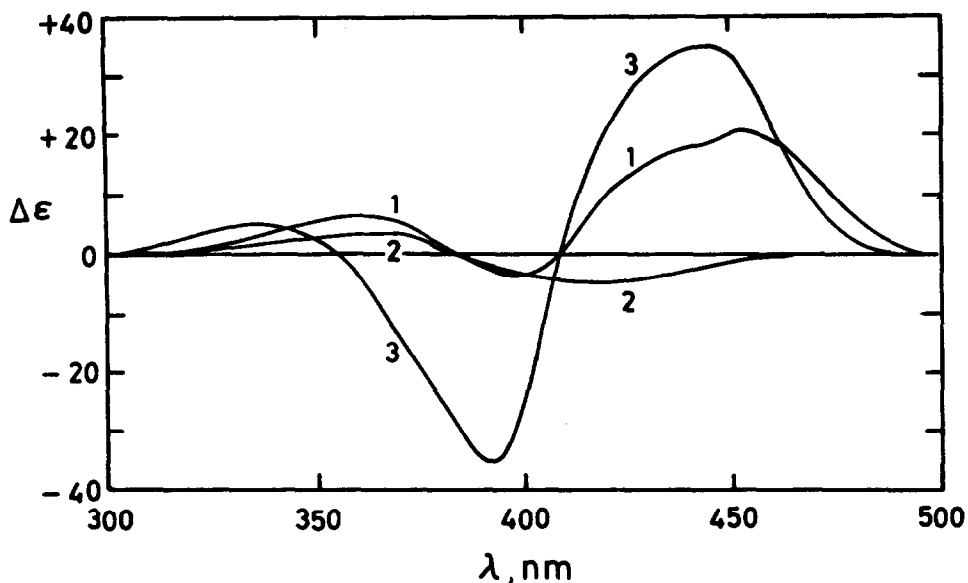


FIGURE 6. Comparison of the circular dichroism (CD) spectra of N_{21},N_{22} and N_{21},N_{24} -methanomesobilirubin-XIII α (1 and 2) (curves 1 and 2, respectively) on human serum albumin (HSA) with mesobilirubin-XIII α on HSA (curve 3) in pH 7.4 Tris buffer containing 1% $(\text{CH}_3)_2\text{SO}$ at 22°C. The concentration of pigment in each spectrum is 2×10^{-6} M and that of HSA is 4×10^{-5} M, for a 1:2 molar ratio of pigment to albumin.

CONCLUDING COMMENTS

Intramolecular hydrogen bonding between propionic acid CO_2H and dipyrinone groups is known to be a dominant, conformation stabilizing force in bilirubin and its analogs.⁶ Our study shows that new and interesting, bilirubin analogs can be prepared by linking either the dipyrinone nitrogens or the lactam nitrogens with a $-\text{CH}_2-$ group. The result is (i) an N_{21},N_{22} -methano-bridged pigment (1) that adopts a ridge-tile shape and is only slightly more polar than the parent unbridged rubin; and (ii) an N_{21},N_{24} -methano-bridged pigment (2) that adopts a doughnut-shape in which the dipyrinones are highly twisted. In the presence of molecular recognition agents, such as HSA, (-)-ephedrine or quinine, 1 exhibits moderate to intense induced bisignate circular dichroism, but 2 exhibits only weak to moderate bisignate CD.

EXPERIMENTAL

General Procedures. Nuclear magnetic resonance (NMR) spectra were determined on a GE QE-300 300-MHz spectrometer in CDCl_3 solvent (unless otherwise specified) and reported in δ ppm downfield from $(\text{CH}_3)_4\text{Si}$. Infrared (IR) spectra were determined on a Perkin-Elmer 1600 Fourier transform spectrophotometer. All ultraviolet-visible spectra were recorded on a Perkin Elmer Model 3840 diode array or Cary 219 spectrophotometer, and all circular dichroism (CD) spectra were recorded on a JASCO J-600 instrument. Melting points were determined on a Mel-Temp capillary apparatus and are uncorrected. Combustion analyses were carried out by Desert Analytics, Tucson, AZ. High resolution mass spectra were run at the Midwest Center for Mass Spectrometry, University of Nebraska, Lincoln. Analytical thin layer chromatography

was carried out on J.T. Baker silica gel IB-F plates (125 μ layer). Flash column chromatography was carried out using Woelm silica gel F, thin layer chromatography grade. Radial chromatography was carried out on Merck Silica gel PF-254 with CaSO₄ preparative thin layer grade, using a Chromatotron (Harrison Research, Inc., Palo Alto, CA). HPLC analyses were carried out on a Perkin-Elmer Series 4 high performance liquid chromatograph with an LC-95 UV-visible spectrophotometric detector (set at 410 nm) equipped with a Beckman-Altex ultrasphere-IP 5 μ m C-18 ODS column (25 x 0.46 cm) and a Beckman ODS precolumn (4.5 x 0.46 cm).¹³ The flow rate was 1.0 mL/minute, and the elution solvent was 0.1 M di-*n*-octylamine acetate in 5% aqueous methanol (pH 7.7, 31°C).

Spectral data were obtained in spectral grade solvents (Aldrich or Fisher). Diiodomethane, tetrahydrofuran, 2-propanol, dichloromethane, dimethylsulfoxide, methyl lithium, sodium methoxide and sodium borohydride were from Aldrich. Tetrahydrofuran was dried by distillation from sodium; methanol was dried (Mg, reflux) and distilled. Solutions of *N*₂₁,*N*₂₂-methanomesobilirubin-XIII α (1), mesobilirubin-XIII α (3) and *N*₂₁,*N*₂₄-methanomesobilirubin-XIII α (3) in pH 7.4 aqueous human serum albumin were prepared as reported earlier,²¹ except the weighed pigment and albumin were mixed together in 0.3 mL of dimethylsulfoxide, cooled in ice, then diluted with Tris buffer to a final volume of 10 mL.

***N*₂₁,*N*₂₂-Methanomesobiliverdin-XIII α Dimethyl Ester (6).** Mesobiliverdin-XIII α dimethyl ester (8)¹¹ (123 mg, 0.2 mmol) was dissolved in dry dimethylsulfoxide (20 mL), methyl lithium (0.54 mL and 1.4 M) was added at room temperature, and the reaction vessel was blanketed with a nitrogen atmosphere. The reaction was heated to 100°C, and the solution was stirred for 10 minutes. Then diiodomethane (0.4 mL) was added to the hot solution dropwise, and stirring was continued for an additional 10 minutes. The hot solution was poured into an ice/water (200 mL) and dichloromethane (30 mL) mixture to quench the reaction. After separation of the organic layer, the aqueous layer was extracted with dichloromethane until it was colorless. The combined organic layers were washed with cold water (3 x 300 mL) then with saturated aqueous sodium chloride solution (100 mL). The washed organic layer was dried over anhydrous sodium sulfate, filtered, and evaporated. Purification of the residue by flash column chromatography gave 16 mg (13% yield) of desired product (eluent: dichloromethane-methanol, 100:3 vol/vol). Verdin 6 had mp 216°C (decomp.); IR (chloroform): ν 3328, 2970, 1755, 1668 cm⁻¹; ¹H-NMR: δ 1.19 (m, 6H), 1.83 (s, 3H), 1.862 (s, 3H), 2.07 (s, 3H), 2.14 (s, 3H), 2.51 (m, 8H), 2.94 (m, 4H), 3.62 (s, 3H), 3.68 (s, 3H), 5.83 (s, 1H), 5.92 (s, 2H), 6.14 (s, 1H), 6.79 (s, 1H), 10.12 (b, 1H) ppm; ¹³C-NMR: δ 9.08 (q), 9.19 (q), 9.45 (q), 10.47 (q), 15.03 (q), 15.09 (q), 18.37 (t), 18.49 (t), 20.74 (t), 21.11 (t), 35.47 (t), 35.91 (t), 52.25 (q), 52.35 (q), 56.69 (t), 96.07 (d), 96.54 (d), 115.6 (d), 122.2 (s), 128.9 (s), 130.1 (s), 131.0 (s), 133.9 (s), 134.7 (s), 136.6 (s), 143.2 (s), 143.9 (s), 145.7 (s), 146.5 (s), 150.9 (s), 168.6 (s), 170.2 (s), 172.6 (s), 173.7 (s), 173.8 (s) ppm.

Anal. Calcd for C₃₆H₄₂N₄O₆: C, 68.99; H, 6.75; N, 8.94.
Found: C, 69.29; H, 6.68; N, 8.95.

***N*₂₁,*N*₂₂-Methanomesobilirubin-XIII α Dimethyl Ester (3).** *N*₂₁,*N*₂₂-Methanomesobiliverdin dimethyl ester (58 mg, 0.092 mmoles) was dissolved in nitrogen-saturated tetrahydrofuran (7 mL) and 2-propanol (7 mL). Then methanol (0.4 mL) and sodium borohydride (40 mg, 1.05 mmoles) were added, and the reaction was stirred for 10 minutes. Another like portion of methanol and sodium borohydride was added and stirring was continued for 2 hours. The reaction was neutralized with 10% aqueous hydrochloric acid. After keeping the mixture at -30°C for 2 hours, a white inorganic salt was removed by filtration and washed with a small amount of dichloromethane. The liquid portion was taken up into dichloromethane and washed with nitrogen-saturated water (3 x 200 mL) and a saturated sodium chloride solution. After drying over anhydrous sodium sulfate, the organic layer was filtered and evaporated. The product mixture was separated chromatographically by radial chromatography on silica gel (2 mm layer) eluting with dichloromethane-methanol, 25:1 vol,vol to give 44 mg (75% yield) of the desired yellow pigment (3). It had mp 172 °C (decomp) IR (chloroform): ν 3340, 2923, 1435, 1668 cm⁻¹; UV-visible data in Table 4; ¹H-NMR: δ 1.15

(m, 6H), 1.832 (s, 3H), 1.86 (s, 3H), 2.07 (s, 3H), 2.08 (s, 3H), 2.25 (s, 2H, $J=7.2$ Hz), 2.46 (m, 6H), 2.62 (t, 2H, $J=7$ Hz), 2.73 (t, 2H, $J=7$ Hz), 3.625 (s, 3H), 3.64 (s, 3H), 4.17 (s, 2H), 5.35 (s, 2H), 6.02 (s, 1H), 6.10 (s, 1H), 9.80 (brs, 1H), 9.905 (brs, 1H) ppm; $^{13}\text{C-NMR}$: δ 8.30 (q), 8.41 (q), 8.94 (q), 9.54 (q), 14.67 (q), 14.85 (q), 17.77 (t), 17.89 (t), 19.75 (t), 19.80 (t), 22.18 (t), 34.53 (t), 34.55 (t), 51.53 (q), 52.00 (q), 54.27 (t), 96.83 (d), 99.46 (d), 118.6 (s), 119.9 (s), 121.1 (s), 123.4 (s), 123.6 (s), 123.8 (s), 123.8 (s), 125.5 (s), 128.8 (s), 128.9 (s), 129.1 (s), 129.9 (s), 143.2 (s), 148.0 (s), 168.9 (s), 173.5 (s), 173.5 (s), 174.3 (s) ppm.

Anal. Calcd for $\text{C}_{36}\text{H}_{44}\text{N}_4\text{O}_6$: C, 68.77; H, 7.05; N, 8.91.

Found: C, 68.49; H, 6.89; N, 8.81.

N_{21},N_{22} ; N_{23},N_{24} -Dimethanomesobilirubin-XIII α Dimethyl Ester (5). Following reduction of N_{21},N_{22} -methanomesobiliverdin dimethyl ester (5) as above, the reaction was quenched with 10% aqueous hydrochloric acid and the pH was adjusted to 3. Continuing with the same work-up, radial chromatography separated 12 mg (20%) of compound 3 and 12 mg (20%) of 4. The dimethano ester (5) had mp 200 °C (decomp); UV-visible data in Table 4; $^1\text{H-NMR}$: δ 1.15 (t, 6H, $J=7.5$ Hz), 1.90 (s, 3H), 2.08 (s, 3H), 2.43 (m, 8H), 2.71 (t, 4H), 3.65 (s, 6H), 4.10 (s, 2H), 5.29 (s, 4H), 6.09 (s, 2H) ppm; $^{13}\text{C-nmr}$: δ 8.34 (q), 8.97 (q), 14.66 (q), 17.79 (t), 19.79 (t), 20.71 (t), 34.64 (t), 51.62 (q), 54.19 (t), 96.79 (d), 118.4 (s), 121.7 (s), 124.2 (s), 125.7 (s), 127.1 (s), 130.1 (s), 143.4 (s), 168.9 (s), 175.1 (s) ppm. High resolution mass spectral analysis: Calcd for $\text{C}_{37}\text{H}_{44}\text{N}_4\text{O}_6$: 640.3261. Found: 640.3268.

N_{21},N_{22} -Methanomesobilirubin-XIII α (1). N_{21},N_{22} -Methanomesobilirubin-XIII α dimethyl ester (10 mg, 0.016 mmoles) was added to a solution of 2 *N* aqueous sodium hydroxide (3 mL, nitrogen-saturated) in ethanol (5 mL, nitrogen-saturated) and heated at reflux for 3 hours under nitrogen atmosphere in the dark. After cooling the reaction to room temperature, the ethanol was removed by evaporation, and the residue was dissolved in water. To remove unreacted ester, the yellow solution was washed with dichloromethane until the organic layer became colorless. The temperature of the aqueous solution was reduced to 0–5 °C using an ice bath. Following careful addition of 10% aqueous hydrochloric acid to adjust the pH to 7, a yellow precipitate formed. The mixture was extracted with dichloromethane until colorless. The combined organic layers were washed with cold, degassed water (3 x 50 mL) and saturated sodium chloride solution, then dried over anhydrous sodium sulfate, filtered and evaporated. Following the addition of methanol (5 mL) in an ultrasonic bath, a bright yellow solid could be recovered. After keeping the mixture at -15 °C overnight, the solid was filtered and dried under vacuum. Further purification was achieved by radial chromatography on silica gel (1 mm layer) eluting with dichloromethane-methanol, 100:4 vol,vol to give 8 mg (80% yield) of 1. It had mp 215° (decomp); IR (chloroform): ν 3321, 2953, 1731, 1688 cm^{-1} ; UV-visible data in Table 4; $^1\text{H-NMR}$: δ 1.13 (t, 6H, $J=7.5$ Hz), 1.86 (s, 3H), 1.87 (s, 3H), 2.18 (s, 3H), 2.16 (s, 3H), 2.48 (q, 4H, 7.5 Hz), 2.567–3.13 (broad multiple signal), 4.08 (b, 1H), 4.13 (b, 1H), 4.79 (b, 1H), 5.84 (b < 1H), 6.09 (s, 1H), 6.20 (s, 1H), 8.15 (s, 1H), 10.81 (s, 1H), 11.99 (b, 1H), 13.6 (b, 1H) ppm; $^{13}\text{C-NMR}$ data in Table 1.

Anal. Calcd. for $\text{C}_{34}\text{H}_{40}\text{O}_6\text{N}_4$ (600.72): C, 67.98; H, 6.71; N, 9.33.

Found: C, 68.17; H, 6.53; N, 9.02.

N_{21},N_{24} -Methanomesobilirubin-XIII α (2) was prepared from 8 as in Scheme 1 and described previously.¹²

Molecular Dynamics. Conformational energy maps for and molecular modelling of the pigments of this work follow from molecular mechanics calculations carried out on an Evans and Sutherland ESV-10 workstation using version 6.0 of SYBYL (Tripos Assoc., St. Louis, MO) as described earlier.⁶ The conformational energy maps were created using Wingz™ (Informix), and the ball and stick drawings were created

from the atomic coordinates of the molecular dynamics structures using Müller and Falk's "Ball and Stick" program (Cherwell Scientific, Oxford, U.K.) for the Macintosh.

Acknowledgements. We thank the National Institutes of Health (HD17779) for generous support.

REFERENCES AND NOTES

1. McDonagh, A. F. In *The Porphyrins*; Dolphin, D., Ed., Academic Press: New York, 1979; Vol. 6, pp 293-491.
2. For leading references, see Ostrow, J. D., Ed. *Bile Pigments and Jaundice*; Marcel-Dekker: New York, 1986.
3. Falk, H. *The Chemistry of Linear Oligopyrroles and Bile Pigments*; Springer Verlag: New York, 1989.
- 4.(a) Bonnett, R.; Davies, J. E.; Hursthouse, M. B.; Sheldrick, G. M. *Proc. R. Soc. London, Ser. B*, **1978**, *202*, 249-268.
(b) LeBas, G.; Allegret, A.; Mauguen, Y.; DeRango, C.; Bailly, M. *Acta Crystallogr., Sect. B*, **1980**, *B36*, 3007-3011.
(c) Becker, W.; Sheldrick, W. S. *Acta Crystallogr., Sect. B*, **1978**, *B34*, 1298-1304.
- 5.(a) Kaplan, D.; Navon, G. *Isr. J. Chem.*, **1983**, *23*, 177-186.
(b) Kaplan, D.; Navon, G. *Org. Magn. Res.*, **1981**, *17*, 79-87.
(c) Kaplan, D.; Navon, G. *Biochem. J.*, **1982**, *201*, 605-613.
(d) Navon, G.; Frank, S.; Kaplan, D. *J. Chem. Soc. Perkin Trans. 2*, **1984**, 1145-1149.
(e) Manitto, P.; Monti, D. *J. C. S. Chem. Commun.*, **1976**, 122-123.
6. Person, R.V.; Peterson, B.R.; Lightner, D.A. *J. Am. Chem. Soc.*, **1993**, *116*, 42-59.
7. McDonagh, A.F.; Lightner, D.A. In *Hepatic Metabolism and Disposition of Endo and Xenobiotics* (Falk Symposium No. 57, Bock, K.W.; Gerok, W.; Matern, S., eds.) Kluwer, Dordrecht, The Netherlands, **1991**, Chap. 5, pp 47-59.
8. Blanckaert, N.; Heirwegh, K.P.M.; Zaman, Z. *Biochem. J.*, **1977**, *164*, 229-236.
- 9.(a) Lightner, D.A.; McDonagh, A.F. *Accounts Chem. Res.*, **1984**, *17*, 417-424.
(b) McDonagh, A.F.; Lightner, D.A. *Pediatrics*, **1985**, *75*, 443-455.
10. Falk, H.; Thirring, K. *Tetrahedron*, **1981**, *37*, 761-766.
11. Shrouf, D.P.; Puzicha, G.; Lightner, D.A. *Synthesis*, **1992**, 328-332.
12. Hwang, K.O.; Lightner, D.A. *Heterocycles*, **1994**, *37*, 804-814.
13. McDonagh, A.F.; Palma, L.A.; Lightner, D.A. *J. Am. Chem. Soc.*, **1982**, *104*, 6867-6869.
14. Trull, F.R.; Ma, J.S.; Landen, G.L.; Lightner, D.A. *Isr. J. Chem.*, **1983**, *23*, 211-218.
- 15.(a) Lightner, D.A.; Trull, F.R. *Spectrosc. Lett.*, **1983**, *16*, 785-803.
(b) Lightner, D.A.; Ma, J-S. *Spectrosc. Lett.*, **1984**, *17*, 317-327.
- 16.(a) Lightner, D.A.; Ma, J-S.; Adams, T.C.; Franklin, R.W.; Landen, G.L. *J. Heterocyclic Chem.*, **1984**, *21*, 139-144.
(b) Trull, F.R.; Franklin, R.W.; Lightner, D.A. *J. Heterocyclic Chem.*, **1987**, *24*, 1573-1579.
17. Lightner, D.A.; Gawrofski, J.; Wijekoon, W.M.D. *J. Am. Chem. Soc.*, **1987**, *109*, 6354-6362.
- 18.(a) Harada, N.; Nakanishi, K. *Circular Dichroic Spectroscopy - Exciton Coupling in Organic Stereochemistry*; University Science Books: Mill Valley, CA, 1983.
(b) Kasha, M.; Rawls, H.R.; El-Bayoumi, M.A. *Pure Appl. Chem.*, **1965**, *32*, 371-392.
19. Falk, H.; Schliederer, T.; Wohlschann, P. *Monatsh. Chem.*, **1981**, *112*, 199-207.
20. Lightner, D.A.; Wijekoon, W.M.D.; Zhang, M.H. *J. Biol. Chem.*, **1988**, *263*, 16669-16676.
- 21.(a) Blauer, G. *Isr. J. Chem.*, **1983**, *23*, 201-209 and references therein.
(b) Hartz, D.; Blauer, G. *Arch. Biochem. Biophys.*, **1975**, *170*, 375-386.

(Received in USA 4 April 1994; accepted 24 June 1994)